ELSEVIER

Journal of Nuclear Materials 241-243 (1997) 755-759

journal of nuclear materials

Radiative plasmas in TdeV

B. Terreault *,[1], N. Richard [2], J. Mailloux [1], G. Abel [1], C. Côté [3], E. Haddad [2], W. Zhang [1,4], C. Boucher [1], S. Chiu [1], J. Gunn [1], H.H. Mai [1], F. Meo [1], B.L. Stansfield [1], W.W. Zuzak [1]

Centre canadien de fusion magnétique, 1804 Boulevard Lionel-Boulet, Varennes, Que., Canada J3X 1S1

Abstract

The main aspects of radiative plasma experiments carried out in the LH-heated TdeV tokamak are summarized. D_2, N_2 and Ne puffing, and divertor biasing, are assessed in terms of their ability to increase edge and divertor radiative losses and reduce neutralizer plate heat loads. Detailed patterns of radiation and plate power deposition are compared. Combined N_2 and D_2 puffing gives the best results. Biasing enhances divertor radiation but also causes an increase in power conducted and convected to one of the divertor legs. The improvements obtained are still insufficient due to disruptive instabilities that appear at high impurity puffing rates. The instability is triggered at the edge with N_2 and in the core with Ne.

Keywords: Radiation symmetry; Energy deposition; Disruptions; Poloidal divertor; Biasing

1. Introduction

We summarize the main aspects of the experiments carried out on the TdeV tokamak in order to reduce the power loads on the divertor plates. D_2, N_2 and Ne puffing, divertor biasing and combinations of those were used in attempts to enhance the radiative losses from the outer shell of the main plasma and/or the divertor region, without increasing radiation from the plasma core, diluting the fuel, or causing instabilities. In the limiter tokamak TEXTOR, a series of experiments have already shown that neon injection could produce a highly radiative peripheral layer, at a power level of 4 MW (NBI and ICRF), keeping Z_{eff} low, and with improvement of confinement over L-mode [1,2]. In the large open divertor tokamaks ASDEX Upgrade [3], DIII-D [4], JET [5] and JT60-U [6] with very high levels of auxiliary heating (7 to 28 MW, mostly NBI), injection of N_2, Ne or Ar has been successful in reducing drastically the divertor plate power loads, but at the cost of unacceptably high Z_{eff} (typically 3), and some degradation of confinement with respect to ELMy H-mode scaling. It is hoped that better impurity retention with closed divertors will remedy these deficiencies.

TdeV, in addition to having closed divertors, allows divertor biasing which has been shown to improve particle retention and enhance the hydrogenic divertor radiation [7]. TdeV is heated by LH waves (< 1 MW). First, we give a comparison of the detailed spatial distributions of the radiation and the conduction and convection losses in the different regimes. Interesting scenarios all involve plasma detachment, with a line-average density around 6×10^{19} m^{-3}, but the spatial patterns differ very significantly. Secondly, we discuss the disruptive instabilities that limit the acceptable impurity injection rates.

2. Experiments

The results refer to similar L-mode plasmas with $B_T = 1.8$ T, $I_P = 190$ kA, $R = 0.86$ m, $a = 0.26$ m, $q_{cyl} = 3.7$, upper single null, ion ∇B drift away from X-point, and strike point in the middle of the horizontal neutralizer plates. A drawing of the TdeV divertor is shown in Fig. 1. The inner and horizontal outer divertor plates can be

* Corresponding author. Tel.: +1-514 652 8693; fax: +1-514 652 8625; e-mail: terreault@ccfm.ireq.ca.

[1] INRS-Énergie et Matériaux, Université du Québec.

[2] MPB Technologies, Inc.

[3] Consultants ProTek.

[4] Present address: Jet Joint Undertaking.

PII S0022-3115(96)00601-0

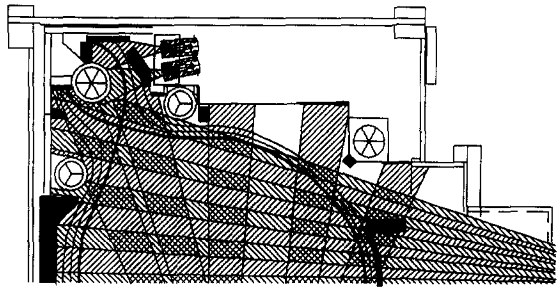

Fig. 1. Poloidal section of the upper half of TdeV showing the divertor geometry and the lines of sight of the bolometry system (slashes). Plasma interacting surfaces are shaded in solid black.

biased; the oblique plates are grounded and cover only 1/3 of the toroidal circumference. N_2 and Ne have been injected uniformly in the cryopumped divertor through 6 fast piezo valves; Ne was also introduced as a short puff, with divertor pumps off. The plasma was heated by 550 kW of 3.7 GHz LH power. This represents the non-reflected power, but the precise fraction absorbed in the main plasma is not known because LH wave absorption mechanisms at high density are not well understood. Whereas 90–100% of the input power is accounted for as radiation or surface deposited power in Ohmic plasmas, with LH heating only 70–80% is measured. A sizeable part is directly coupled to the SOL [8]. The main diagnostics used are: (1) Bolometer arrays, shown in Fig. 1, with typical spatial resolution of 3 cm; a wide angle detector also measures the total power radiated in the main plasma including X-point; (2) 64 thermocouples located in divertor plates (2 or 3 per plate) at several toroidal locations, in the divertor baffle, in limiters and in the LH antenna [8]; (3) an infrared camera viewing inner and outer divertor (0.2 m × 0.2 m area, 1 mm/pixel); (4) soft X-ray (SXR) tomography (20 mm resolution); (5) UV spectroscopy (7 chords, resolution of 40 mm at edge and 80 mm in center); (6) 'Z_{eff} meter' based on central bremsstrahlung radiation at a wavelength of 5235 ± 5 nm.

3. Power balance in enhanced radiation regimes

Fig. 2 compares relevant traces for the plasma evolution under simple D_2 puffing and combined D_2 plus N_2 puffing. Full LH power is applied from 350 ms on, and the N_2 injected at the rate of 8.5×10^{20} atom/s after 425 ms; witness the central and edge NV line emission. With N_2, the central SXRs are slightly enhanced but loop voltage, Z_{eff}, and main plasma radiation (including X-point) remain the same. On the other hand, the radiative losses from the X-point region itself are approximately doubled. (The inner divertor is lumped with the X-point radiation because of inadequate resolution for true 2D bolometric tomogra-

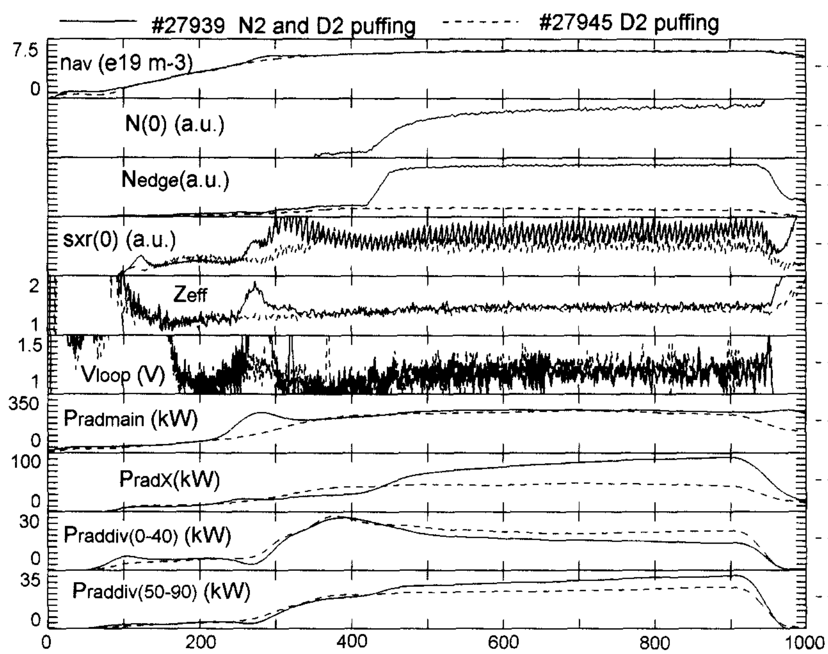

Fig. 2. Two stable detached shots, one with D_2 puffing in the main chamber (#27945, dashed traces), one with also N_2 puffing in the divertor (#27939, solid traces). The signals shown are the line-average density, the NV (123.8 nm) intensities viewed inside the $r = 0.08$ m tangency radius and outside $r = 0.22$ m, central SXRs, Z_{eff}, loop voltage, main plasma radiated power (signal Pradmain *includes* X-point), X-point and inner divertor radiation, and outer divertor radiation 0–40 mm from the plates and 50–90 mm from the plates towards the X-point.

phy.) Also, the radiation from the immediate vicinity (0–40 mm) of the outer divertor plate is reduced, while that from the midway region (50–90 mm) increases. These facts indicate, first, a more pronounced detachment [9] with N_2, second, satisfactory N retention in the divertor [10], and last, that N radiates away from the plasma core under the present conditions. In this respect, the peak in the radiation coefficient $L(T_e)$ is around 10 eV for N ions, assuming coronal equilibrium [5]; including transport effects, this peak is shifted to about 25 eV in TdeV [11], a typical separatrix electron temperature in TdeV at high density. Thus N appears to be an ideal radiator for TdeV. However, the radiation cannot be enhanced further by more intense puffing because the plasma becomes unstable.

Fig. 3 displays details of the power balance for the different scenarios. A preliminary remark: the OH power increases substantially with puffing because it raises the density from $\approx 3 \times 10^{19}$ m^{-3} to $\approx 6 \times 10^{19}$ m^{-3}, the LH wave no longer drives any significant current, and the loop voltage increases from ≈ 0.4 to ≈ 1.2V. We separate radiation into 'core' ($r < 0.21$ m), 'shell' ($r > 0.21$ m, but excluding X-point vicinity), X-point and inner divertor, and outer divertor near and far from plate. The 'edge' radiation is the sum of shell, X-point and divertor radiation. D_2 puffing and detachment (seen for instance in the shift of divertor radiation from the plate towards the X-point) have the effect of enhancing radiation rather equally in the core and peripheral plasmas. The surface deposited power loads are reduced from 62% to 41% of the measured power. Noticeably, these loads shift outwards, from the inner and horizontal outer plates to the oblique plates and the 'wall', i.e. guard limiters, throat baffle plate and LH antenna. The addition of N_2 does not lead to a significant change in the ratio of radiation to surface deposition, but is very favorable because it shifts the radiation from the core to the X-point region. The MARFE-like radiative 'blob', usually detected in the upper inboard region of the 'shell', is replaced by more stable X-point radiation with N_2. Biasing, without D_2 puffing, doubles the radiation from the X-point and the divertor. It also modifies the distribution of the conducted and convected loads, producing a narrower SOL with the load more concentrated on the horizontal outer plates; it does not alleviate the plate power load problem. Stable neon seeded discharges could only be obtained with the help of biasing; however, the reduction in plate load is obtained at the expense of more core radiation. It may be noted that the Ne radiation coefficient has peaks at ≈ 30 eV and ≈ 300 eV under coronal equilibrium [5], with the first

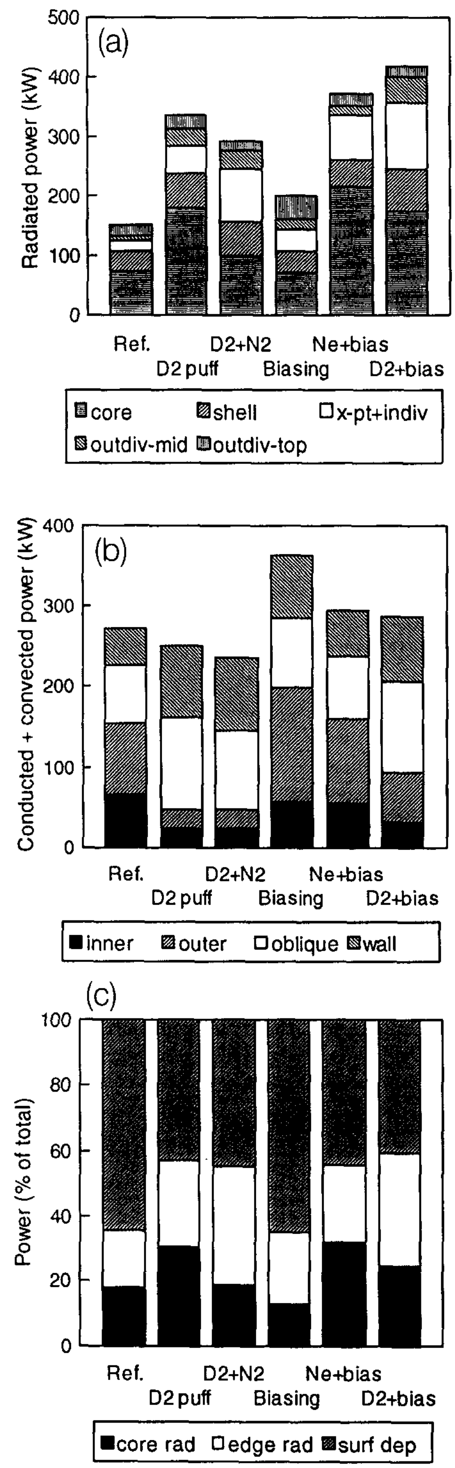

Fig. 3. (a) Distribution of radiation between core, shell, X-point and inner divertor, and outer divertor (near plate and midway to X-point), for reference shot and for different radiative scenarios. (b) Distribution of power deposited on inner, outer and oblique plates, and wall. (c) Partition between core radiation, edge radiation and deposition on surfaces (normalized to total measured power).

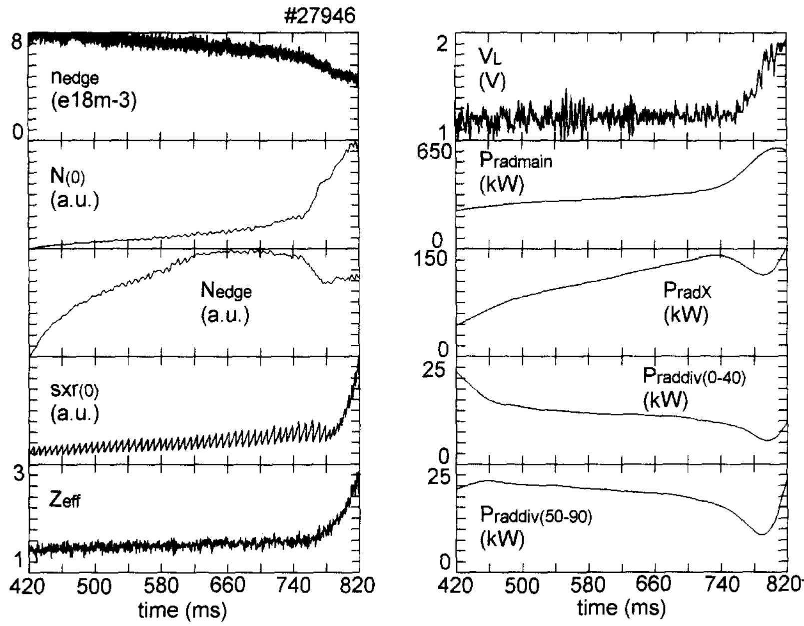

Fig. 4. Evolution of an unstable shot after N_2 injection: edge density, central and edge NV line intensities, central SXRs, Z_{eff}, loop voltage, power radiated in the main chamber, near X-point and in inner divertor, and in outer divertor.

peak shifting to ≈ 100 eV with transport effects [11]. Under the present conditions, the TdeV temperature is too low at high density for Ne edge cooling. Biasing in addition to D_2 puffing enhances radiation but also conduction/convection in the outer divertor. The overall performance in terms of edge radiation versus surface deposition is similar to $D_2 + N_2$ puffing, but the distribution on the plates is less favorable. Combining biasing with N_2 puffing could not be done in the last campaign for technical reasons.

4. Disruptive instabilities

In the best of cases, only 60% of the measured power is radiated in stable discharges. In Fig. 4 we show traces for

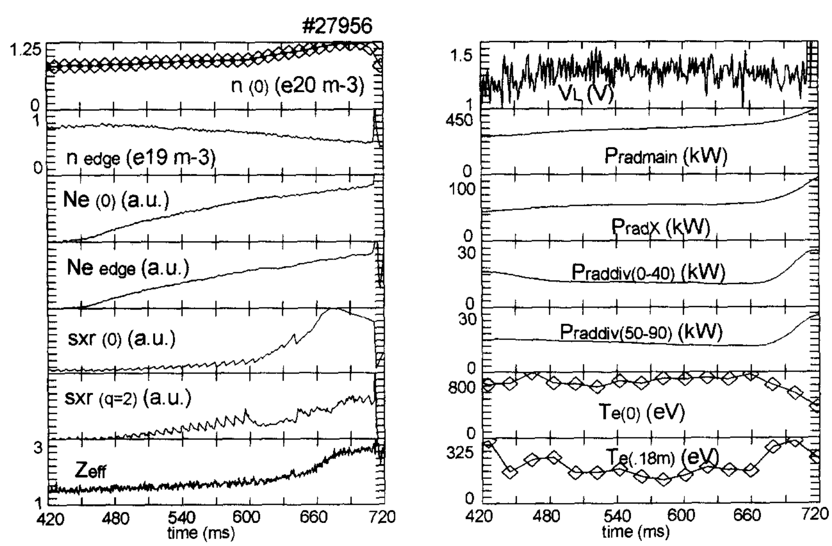

Fig. 5. Evolution of an unstable neon puffing shot: peak and edge densities, central and edge NeVIII line intensities, SXR signals in center and near $q = 2$ surface, Z_{eff}, loop voltage, power radiated in main chamber, X-point and inner divertor, and outer divertor, and electron temperatures in center and at $r = 0.18$ m.

an unstable shot with an N_2 puffing rate of 1.1×10^{21} atom/s, only 30% more than for the shot in Fig. 2, with which it should be compared. We note the peculiar fact that the N atoms at first penetrate only very slowly to the core of the plasma (UV signals). The density and temperature profiles do not differ from those of the shot of Fig. 2, so differences in transport are unlikely. But the N ions accumulate (core NV, SXRs, X-point radiation), until an edge-triggered instability provokes the disruption. We first see a slow decrease in the edge density, and at 750 ms the edge NV signal drops abruptly together with X-point and divertor radiation. At this time, the N ions penetrate catastrophically into the core as witnessed by all diagnostics. The plasma disrupts when the total radiation losses are about equal to the heat input. Although our bolometric system does not have enough chords to show it unambiguously, the instability is probably triggered by a MARFE in the vicinity of the X-point, where the radiation losses reach 150 kW (50% more than in Fig. 2) just before this occurrence. An upgrade of the plasma heating system, providing more usable power, and a feedback on N_2 puffing, to maintain it at an optimal level, should in principle prevent the disruption. Disturbing facts remain, however. Why the poor penetration at first, and the accumulation later? This may imply that the disruption cannot be prevented, only postponed, and is a relevant question for future long pulse tokamaks.

Disruptions with neon injection are in some ways similar and in other ways very different, see Fig. 5. They show, as with N_2, a slow penetration at first, even in the edge, then accumulation. Accordingly, the centrally radiated power and central Z_{eff} increase, slowly at first. The edge density also decreases progressively, but now accompanied by a peaking of the density profile: the ratio of peak to edge density changes from 11 to 25 during the 275 ms following injection (at 425 ms). The SXR intensity increases slowly for the first 175 ms. The sawteeth are particularly violent on the chord with a tangency radius of $r = 132$ mm corresponding to the $q = 2$ surface, indicating efficient transport from the $q = 1$ surface to the $q = 2$ surface (sawtooth propagation time < 0.5 ms). Following a sawtooth crash at $t = 600$ ms, the SXR activity at the $q = 2$ surface drops, while the central SXRs shoot up and the central sawteeth tend to stabilize. All the while, the central Z_{eff} starts increasing more rapidly. At 635 ms, a second transition takes place: the sawteeth are completely stabilized, and the rise of the SXR intensity and Z_{eff} is even more rapid, until at 670 ms the central temperature starts to collapse leading to disruption at $t = 715$ ms. Thus, with neon, an instability inside the $q = 2$ surface is eventually responsible for the disruption.

5. Conclusion

With TdeV heated by LH waves, significant reductions in plate power loads have been achieved, especially with combined D_2 plus N_2 puffing, whereby the X-point radiation is strongly enhanced and the conducted/convected power reduced, while the core radiation actually decreases. However, attempts to increase the radiated fraction above 60% have led to disruptive instabilities that are triggered at the edge with N_2, and inside the $q = 2$ surface with Ne. In both cases, central impurity accumulation takes place. With an upgrade in the auxiliary heating system, the prospects for satisfactory radiative divertor operation with N_2 puffing appear good, whereas the case for neon puffing is not clear. Biasing has contradictory effects; its use in conjunction with N_2 would constitute the test of its usefulness.

Acknowledgements

We thank the whole staff of TdeV for their dedication, and in particular J.-L. Lachambre, M. Gagné and S. Savoie for the biasing and gas systems. The CCFM is funded by the Canadian government, Hydro-Québec and INRS.

References

[1] U. Samm et al., in: Proc. 18th Eur. Conf. Control. Fusion Plasma Phys. (Eur. Phys. Soc., Geneva, 1991) 15C, Part III, p. 157.
[2] A.M. Messiaen et al., Nucl. Fusion 36 (1996) 39.
[3] A. Kallenbach et al., Nucl. Fusion 35 (1995) 1231; Characteristics of radiative boundary discharges with different impurity injection conditions, Report IPP 10/1, MPI für Plasmaphysik, Garching, Germany (Feb. 1996).
[4] S.L. Allen et al., Plasma Phys. Control. Fusion 37 (1995) A191.
[5] JET Team (G.F. Matthews), Plasma Phys. Control. Fusion 37 (1995) A227.
[6] K. Itami et al., Plasma Phys. Control. Fusion 37 (1995) A255.
[7] B. Terreault et al., Nucl. Fusion 34 (1994) 777.
[8] J. Mailloux et al., these Proceedings, p. 745.
[9] B.L. Stansfield et al., these Proceedings, p. 739.
[10] N. Richard et al., these Proceedings, p. 760.
[11] E. Haddad et al., Bull. Am. Phys. Soc. 40 (1995) 1713.